PROCEEDINGS, Twentieth Workshop on Geothermal Reservoir Engineering
Stanford University, Stanford, California, January 24-26 1995
SGP-TR-150

LOCATING AN ACTIVE FAULT ZONE IN COSO GEOTHERMAL FIELD BY ANALYZING SEISMIC GUIDED WAVES FROM MICROEARTHQUAKE DATA

M. Lou[1], P.E. Malin[2] and J.A. Rial[1]

[1]Wave Propagation Lab, Department of Geology, University of North Carolina at Chapel Hill, NC27599-3315

[2]Department of Geology, Duke University, Durham, NC 27708-0235

ABSTRACT

Active fault systems usually provide high-permeability channels for hydrothermal outflow in geothermal fields. Locating such fault systems is of a vital importance to plan geothermal production and injection drilling, since an active fault zone often acts as a fracture-extensive low-velocity wave guide to seismic waves. We have located an active fault zone in the Coso geothermal field, California, by identifying and analyzing a fault-zone trapped Rayleigh-type guided wave from microearthquake data. The wavelet transform is employed to characterize guided-wave's velocity-frequency dispersion, and numerical methods are used to simulate the guided-wave propagation. The modeling calculation suggests that the fault zone is *~200m* wide, and has a P wave velocity of *4.80km/s* and a S wave velocity of *3.00km/s*, which is sandwiched between two half spaces with relatively higher velocities (P wave velocity *5.60km/s*, and S wave velocity *3.20km/s*).

(1) INTRODUCTION

To maintain high-permeability channels for hydrothermal outflow in geothermal fields, it is necessary to have active faults and fractures. In this context, "active" does not indicate that felt earthquakes associated with the fault are imminent, but that there has been enough seismic activity in the geologic past to maintain permeability along the fault plane. From a global survey of active hydrothermal systems, nearly all active venting is closely associated with faults (Aydin and Page 1984, Pollard 1987, Scholz et. al. 1993, Malin 1994). Locating active fault systems is of a vital importance to plan production and injection drilling in a geothermal field, and some major tectonically-controlled fault systems may be mapped directly by surface geological observation or subsurface drilling, or/and indirectly by geophysical methods such as reflection/refraction seismology. However, small to medium scale fault zones are difficult to delineate with traditional seismic reflection/refraction methods, and the surface seismic method is not effective to explore fault zones having vertical or nearly vertical dipping fault planes.

Fault zones usually act as low velocity seismic wave guides. These are energy-trapping, dispersion-inducing channels which make the observation of seismic guided waves an effective tool to delineate and monitor such fault zones. The Love-type fault-trapped seismic guided waves were first discovered in a three-dimensional vertical seismic profiling (VSP) experiment in the area surrounding a borehole drilled into fault zone of the Oroville, California, earthquake of 1975 by Li et. al.(1987). Similar trapped modes were also identified in some of the borehole seismograms obtained at the San Andreas fault near Parkfield (Li et. al. 1990), and at the fault zone of the Landers, California earthquake (Li et. al. 1994). In this paper, we describe how we located an active fault zone in the Coso geothermal field, California, by identifying and analyzing the Rayleigh-type guided waves from microearthquake seismograms recorded by a dense down-hole three-component seismographic network in the Coso area. As far as we know, this is the first report on Rayleigh-type guided waves ever observed in an active fault zone.

The trapped modes in a fault zone arise as a consequence of constructive interference of multiple reflections/ refractions at the boundaries between the low-velocity fault zone and high-velocity surrounding rocks. The waveforms of trapped waves (including features such as amplitude-space distribution and velocity-frequency dispersion) strongly depend on the fault zone geometry and its physical properties. We employed a guided wave modeling method to invert the fault zone width and rock velocity structure. In addition, we used the Wavelet Transform, a kind of time-varying Fourier Transform, to analyze the dispersion and frequency-content of guided wave modes.

(2) GEOLOGIC BACKGROUND AND THE COSO SEISMOGRAPHIC NETWORK

The Coso geothermal field lies to the east of the

Sierra Nevada Frontal Fault (SNFF) in southern Owens Valley, California. The field is covered locally by a thin, less than 100m layer of recent volcanics (Duffield et al. 1980). Geological maps (e.g. Figure 1) of the area (Duffield and Bacon 1981; Roquemore 1981) and recently acquired seismic reflection profiles (Monastero 1992, Malin 1994) delineate the general structure of the area. Although most major NW trending faults exposed on the surface have been detected, their extent below the surface, as well as other possible smaller scale faults systems, have yet to be determined.

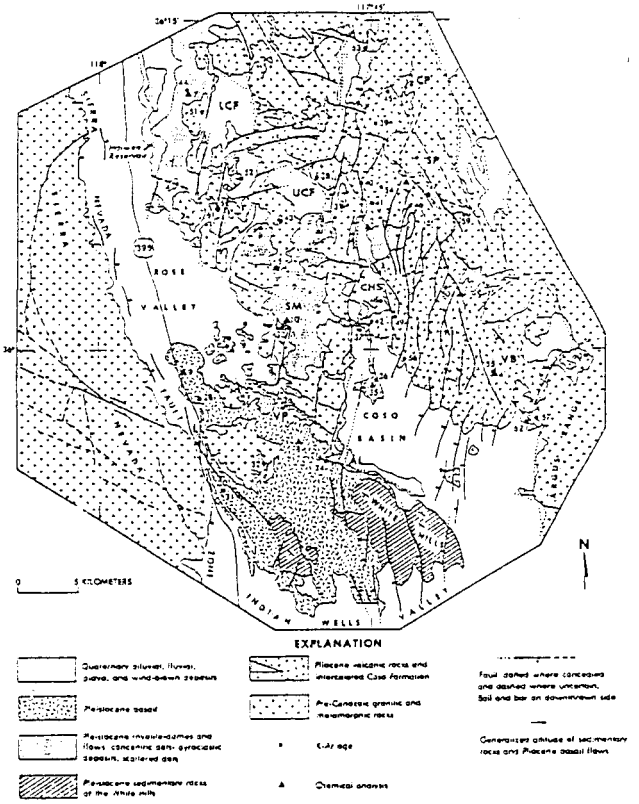

Figure 1. Generalized geological map of the Coso geothermal field and surrounding area (from Duffield and Bacon 1981).

The Coso geothermal area is a very active seismic zone with an average of 20 microearthquakes per day (Malin 1993). Starting in 1990, Duke University has operated a three-component downhole seismographic station network at the area. The network has 16 bit digital telemetry to an earthquake triggered central computer, which samples the signals at 480 Hz. The network sensors are in 100m or deeper boreholes, greatly reducing background noise and increasing the high-frequency band width of microearthquake observations. This downhole sensor environment is particularly useful to record any possible fault-trapped guided waves, since the downhole sensors would avoid the geological complexity of the near surface weathered layer which itself is a low velocity wave guide.

(3)GUIDED WAVE IDENTIFICATION AND ANALYSIS

Figure 2 shows 5 selected seismic stations, laid roughly along a north-south line, which recorded the reported guided waves. Careful inspection of the recently (since July of 1993) recorded events at the 5 stations of Figure 2, revealed that those seismograms recorded at station *S1* with source locations near the dashed line (a possible fault trace with orientation of $\sim N30^{o}W$) display some distinguishing guided-wave features on the components normal to the direction of wave propagation. Figure 3 shows three-component recordings at the same five stations from event *149*,

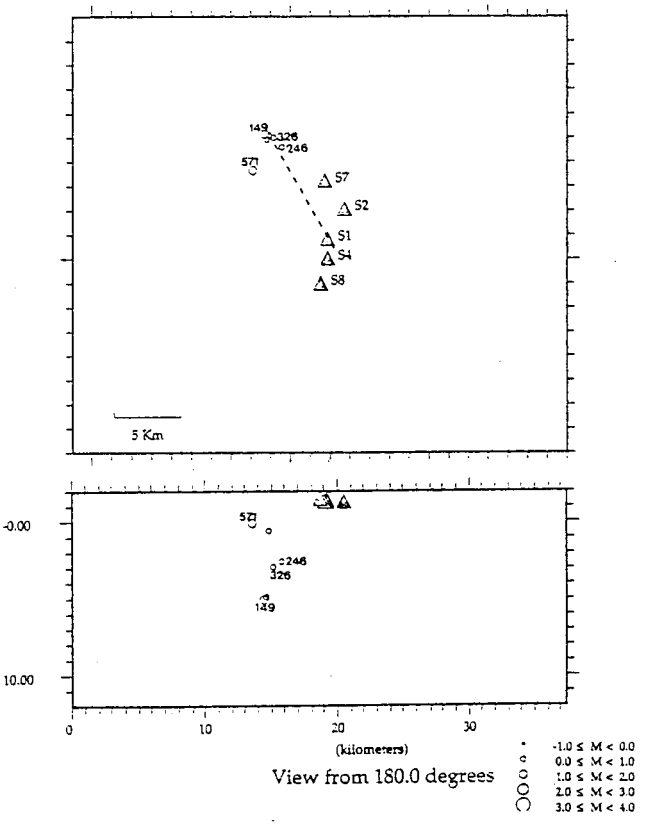

Figure 2. Five selected Coso seismographic network stations, microearthquake event locations, and orientation of a possible active fault zone (dashed line).

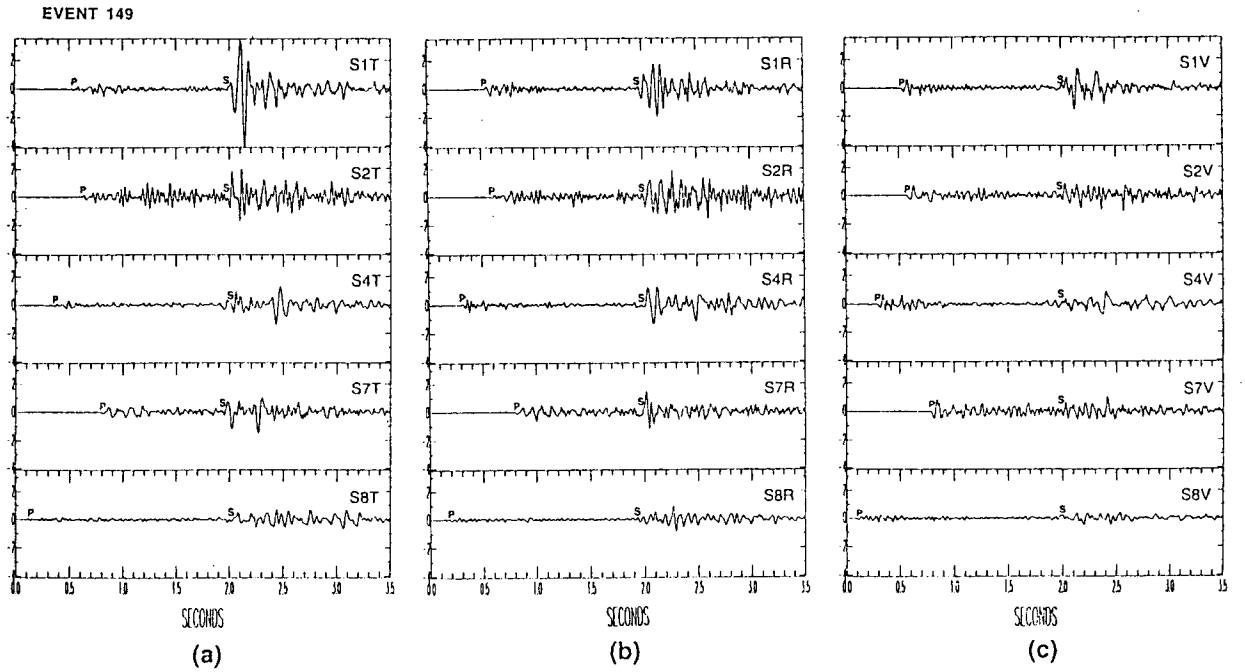

Figure 3. Three-component seismograms of event *149* (inside fault zone) recorded by the five selected stations: (a) the horizontal components normal to propagation direction*(T)* , (b) the horizontal components parallel to propagation direction*(R)* , and (c) the vertical components *(V)*. A large amplitude, dispersive Rayleigh guided wave is received by the two horizontal components of station *S1*, only.

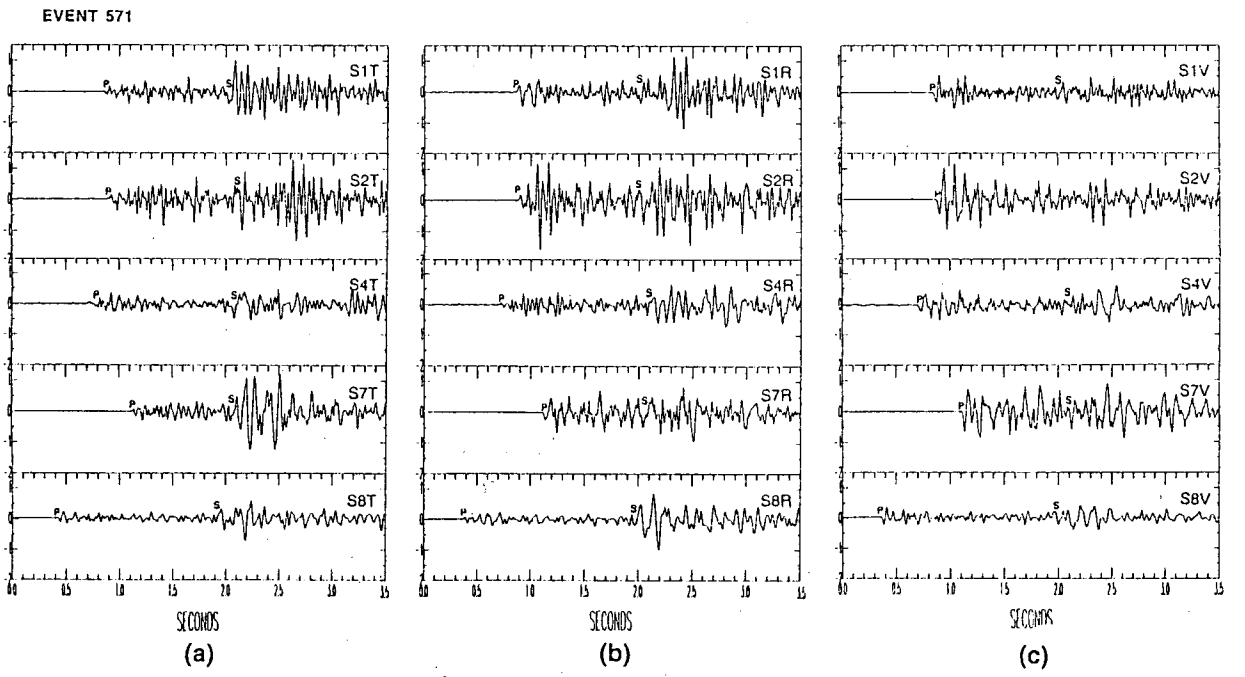

Figure 4. Three-component seismograms of event *571* (outside fault zone) recorded by the five selected stations. (a) the horizontal components normal to propagation direction*(T)*, (b) the horizontal components parallel to propagation direction*(R)*, and (c) the vertical components*(V)*. No guided waves similar to Figure 3 are received by any of the five stations.

which is located at *6.31 km* deep and is of magnitude *1.2*. The seismograms at station *S1*, particularly on the component normal to the direction of wave propagation *(S1T)*, show an abnormally large amplitude and a relatively long period wave train closely following the S wave arrival. The wave train disappears at other stations as located off the dashed line of Figure 2. For example, although station *S7* is at a closer distance(about *9.0km*) from the event than station *S1* (about *12.0km*), the amplitude ratio between components *S1T* and *S7T* is *4:1*. The wave train recorded by the two horizontal components of station *S1* also shows some normal dispersion, which is diagnostic of guided-wave modes. Comparing with the Love-type fault-trapped modes at vertical components observed by Li et. al. (1987, 1990, 1994), the wave train recorded by station *S1* is of Rayleigh type, since it is primarily polarized on the plane normal to a fault plane.

In contrast, the event *571* (*1.36km* deep, magnitude *1.1*) occurring outside the dashed line shows no evidence of a trapped mode at any of the five stations (Figure 4). This suggests that the abnormally large amplitude and relatively long period wave train seen at station *S1* (Figure 3a) is closely associated with the location of the event, rather than with any possible difference of station site effects.

Further evidence for identification of guided waves is shown in the seismograms from two additional fault-zone events *326* (Figure 5a) and *246* (Figure 5b), recorded at the *T*-component of three different stations (*S1, S2, S4)*. The dispersion of guided waves can be easily displayed by a wavelet transform (see Lou and Rial 1995a) shown in Figure 6, for (a) the guided wave recorded by *S1*, and (b) non-guided wave recorded by *S4*, respectively. Typical normal dispersion is seen clearly in Figure 6a, while Figure 6b shows no evidence of dispersion (Indeed, a slightly abnormal dispersion is observed, which may be due to some high frequency attenuation of a body wave).

The source locations and magnitudes of all events showing similar guided-wave characteristics are plotted in Figure 2. The event location distribution suggests that the fault zone has a near vertical fault plane, with the depth extended at least *7 km* below the surface.

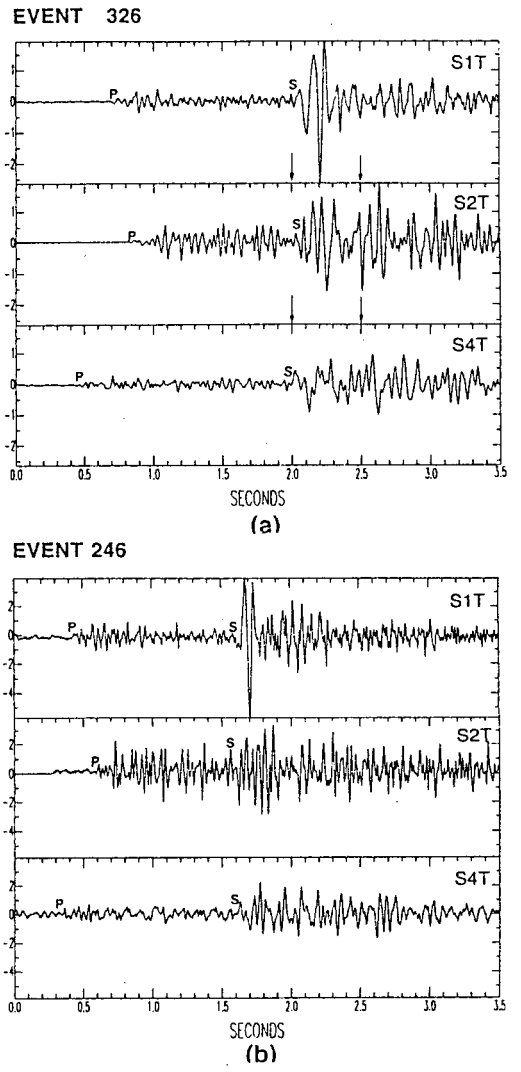

Figure 5. Seismograms of two additional fault-zone events (a) *326* and (b) *246*, recorded by the horizontal component normal to propagation direction of three different stations (*S1T, S2T,* and *S4T)*. A large amplitude, and strong dispersive Rayleigh guided wave is observed by the station *S1* for both events.

(4) GUIDED-WAVE MODELING

To model the above observed seismic guided waves, we employed a Green's function method to compute the Rayleigh guided-wave propagation (Lou and Rial 1995b). Based on plausible seismic velocity structures in the Coso area (Malin 1993, 1994), we constructed a simple fault zone model composed of a low-velocity layer sandwiched between two half-spaces with relatively high P velocity, as shown in Figure 7. Because of the observed guided waves in Figures 3 and 5 have a relative simple, short wave train, we only considered the

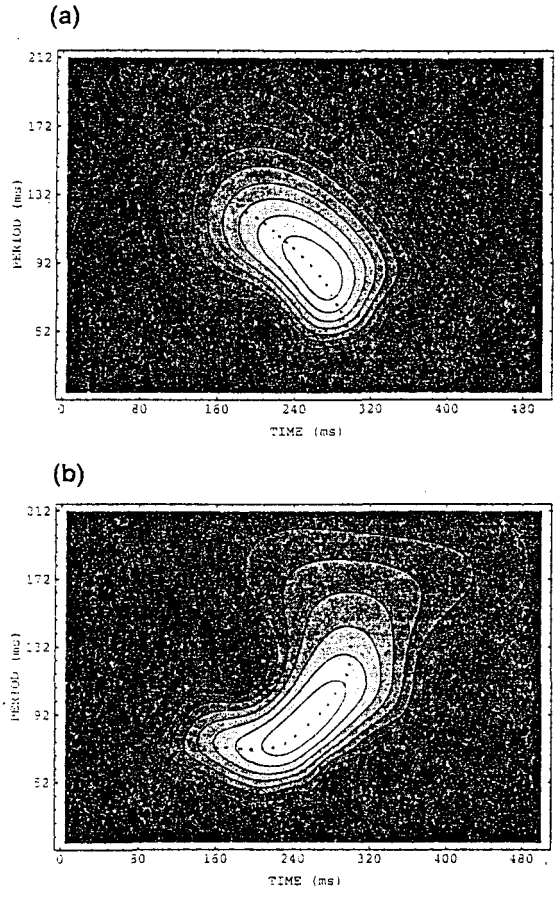

Figure 6. The amplitude spectral of the wavelet transform (a kind of Time-Varying Fourier Transform) to the windowed seismograms of Figure 5a (marked by arrows): (a) the spectrum of the guided wave recorded by the station *S1*, and (b) the spectrum of non-guided wave recorded by the station *S2*.

fundamental mode of Rayleigh-type guided waves. Figure 8 shows the phase-velocity (solid line) and group-velocity (dashed line) dispersion curves of the fundamental mode of Rayleigh guide wave for the fault-zone model of Figure 7. From the group-velocity dispersion curve, we see that the dispersion of the guided wave starts at about *5 Hz*, and is well developed at around *10 Hz*, which basically matches the wavelet transform plot of the observed guided wave in Figure 6a.

Figure 9 illustrates the synthetic results (*synS1T, synS1R, synS4T, and synS4R)* from the simulation of the two-horizontal component seismograms recorded at stations *S1* (inside fault zone) and *S4* (off fault zone) for event *149*. We tested a range of model parameters (fault zone width, P- and S wave velocities), we found the best match to observations with model parameters shown in Figure 7. Although these modeling parameters may not be unique, we think it is reasonable to constrain the velocities on the basis of observed P- and S arrival times, and the width on the period of dispersive trapped waveforms.

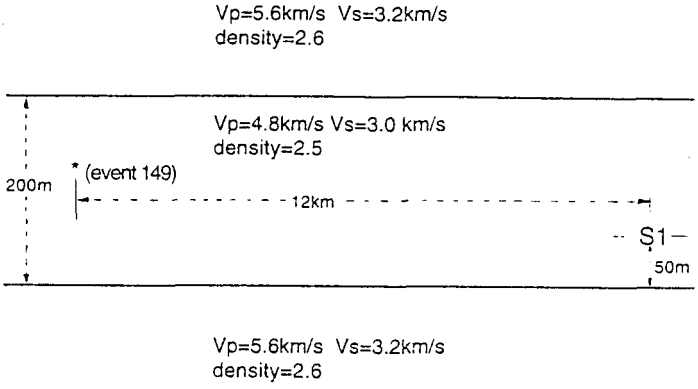

Figure 7. The fault zone model, showing source and station location used to compute the guided wave of event *149*.

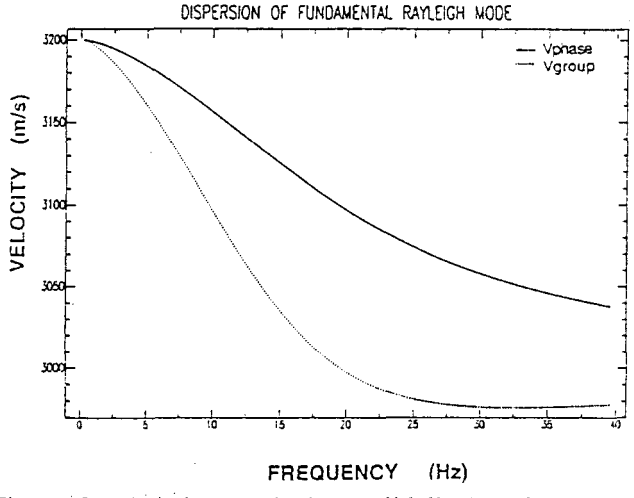

Figure 8. The phase velocity (solid line) and group velocity (dashed line) dispersion curves of the fundamental Rayleigh mode of the guided waves for the model of Figure 7.

We did not include an attenuation factor (internal friction) in the simulation, but simulated it by low-pass filtering (with *15 Hz* high cutoff) the synthetic guided waves. On the other hand, the modeling is somewhat restricted because we only simulated the trapped mode from one event, and we also assumed the fault zone to be a two dimensional infinite uniform waveguide. A more thorough modeling of trapped waves from more events with different locations would result

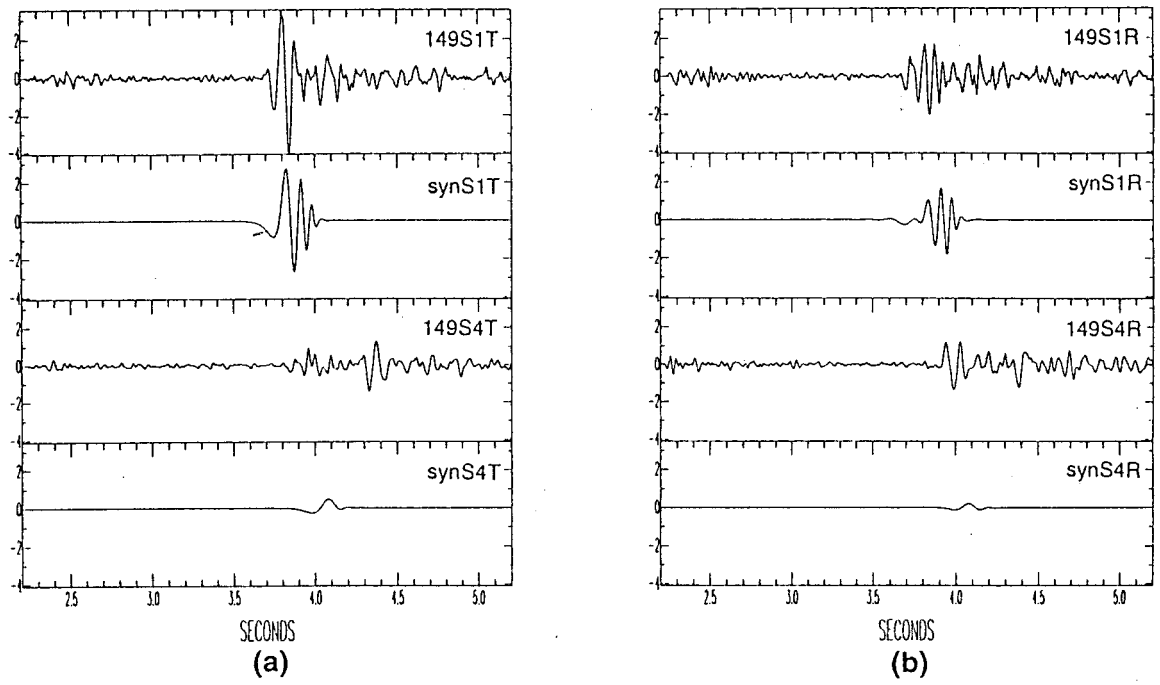

Figure 9. Synthetic guided waves and their comparison with real records of event *149* for two stations *S1* (inside fault zone) and *S4* (outside fault zone): (a) the horizontal component normal to propagation direction, and (b) the horizontal component parallel to propagation direction.

in a more detailed 3-D model of the fault zone. Numerical methods such as finite elements and finite differences, which allow to incorporate some inhomogeneity and intrinsic attenuation, may give more precise modeling results.

(5) DISCUSSION

We have clearly identified a fault-zone trapped Rayleigh-type guided wave from the microearthquake data recorded in the Coso geothermal field, California. As far as we know, this is the first report on a Rayleigh guided-wave ever observed in a fault zone. These trapped modes appear as wave trains of relatively large amplitude wave trains closely following S waves on seismograms recorded at stations close to fault trace for the events occurring within the fault zone. They are clearer on the components normal to fault plane than parallel to fault plane, which suggests the guided waves are of Rayleigh type. For the events occurring in a relatively shallow depth , we also observe strongly dispersive guided waves. From the spectral amplitude of the wavelet transform, we observed that the dominant frequency of trapped mode is lower *(~10Hz)* than the non-guided waves outside fault zone *(~12 Hz*), which is the phenomenon also found by Li et. al. (1987, 1990, 1994).

In order to define the fault zone revealed by those guided waves, we used a numerical method to calculate synthetic Rayleigh-type guided waves. By comparing the observed waveform with the synthetic calculated in a planar low-velocity zone, we estimate a fault zone width of *-200m*, a fault zone P wave velocity of *4.8 km/s* and S wave velocity of *3.0 km/s*, with surrounding rock P wave velocity of *5.6 km /s* and S wave velocity of *3.2km/s*. These parameters are generally consistent with the Coso geologic structure and previous seismic interpretation (Caruso and Malin 1994, Malin 1994). From the source location distribution of guided waves, we estimate the fault system has a near-vertical dip with the depth extended to at least *7 km* below surface.

An active fault system plays a very important role in the development and maintenance of fluid conduits in a geothermal field. Locating such fault system is critic to economically plan production and injection drilling for geothermal reservoirs. The seismic guided waves are very sensitive to the structure and material or fracture properties of an active fault zone. Our work suggests that careful analysis and modeling of such seismic guided

waves could provide a very effective method to locate and monitor active fault systems.

ACKNOWLEDGMENTS

This research is supported by the US Navy (Geothermal Program Office, Naval Air Weapons Station, China Lake), Idaho National Engineering Laboratory (EG&G), the California Energy Company, Inc. (CECI), and the Department of Energy (Geothermal Division), under subcontract No. C93-160437. Authors would like to thank John Copp, CECI for his valuable comments and suggestions to the manuscript.

REFERENCES

Aydin, A. and Page, B. M., 1984, Diverse Pliocence-Quaternary tectonics in a transform environment, San Franscisco Bay region, California: *Geological Society of America Bulletin*, **95**, 1303-1317.

Caruso, C.W. and Malin, P.E., 1994, Shallow structure of the Coso geothermal field, southern Owens Valley, California from high resolution seismic refraction data, *Geophysical Research Letter*, in review.

Duffield, W.A., Bacon, C.R. and Dalrymple, G.B., 1980, Late Cenozoic volcanism, geochronogy, and structure of the Coso Range, Inyo County, California: *Journal of Geophysical Research*, **85**, 2381-2404.

Duffied, W.A. and Bacon, C.R., 1981, Geological map of the Coso volcanic field and adjacent areas, Inyo County, California, *U.S. Geological Survey Miscellaneous Investigations* I -1200.

Li, Y.-G. and Leary, P.C., 1990, Fault zone trapped seismic waves, *Bulletin of Seismology Society of America*, **80**, 1254-1271.

Li, Y.-G., Leary, P.C., Aki, K. and Malin, P.E., 1990, Seismic trapped modes in the Oroville and San Andreas fault zones, *Science*, **249**, 763-766.

Li, Y.-G., Aki, K., Adams, D., Hasemi, A., and Lee, W.H., 1994, Seismic guided waves trapped in the fault zone of the Landers, California, earthquake of 1992, *Journal of Geophysical Research*, **99**, 11705-11722.

Lou, M. and Rial, J.A., 1995a, Application of the wavelet transform in detecting multievents of microearthquake, submitted to the *Geophysical Research Letters*.

Lou, M. and Rial, J.A., 1995b, A numerical method to simulate seismic guided waves, in preparation.

Malin, P.E., 1993, Report on workshop on extensional process in the Coso and Indian Wells Valley area, July 23, 1993, Duke University.

Malin, P.E., 1994, The seismology of extensional hydrothermal system, Geothermal Resources Council TRANSACTIONS, vol.18, 17-22.

Monastero, F.C., 1992, Tectonic influence on geothermal resources in the southwestern Basin and Range, U.S.A.: *China Lake Naval Weapons Center Miscellaneous Reports*.

Pollard, D.D., 1987, Elementary fracture mechanics applied to the structured interpretation of dikes, in Halls, H.C. and Fahrig, W.F., eds., Mafic Dyke Swarms: *Geological Association of Canada Special Paper*, 5-24.

Roquemore, G.R., 1981, Active faults and associated tectonic stress in the Coso Range, California, *Naval Weapons Center Technical Publication* 6270.

Scholz, C.H., Dawers, N.H., Yu, J.Z., Andrers, M.H. and Cowie,P.A., 1993, Fault growth and fault scaling laws: Preliminary results: *Journal of Geophysical Research*, **98**, 21951-21961.